Journal of Crystal Growth 310 (2008) 4871–4875

Contents lists available at ScienceDirect

Journal of Crystal Growth

journal homepage: www.elsevier.com/locate/jcrysgro

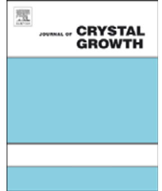

High-reflectivity ultraviolet AlN/AlGaN distributed Bragg reflectors grown by metalorganic chemical vapor deposition

Jun-Rong Chen, Shih-Chun Ling, Chin-Tsang Hung, Tsung-Shine Ko, Tien-Chang Lu *, Hao-Chung Kuo, Shing-Chung Wang

Department of Photonics & Institute of Electro-Optical Engineering, National Chiao Tung University, 1001 University Road, Hsinchu 30050, Taiwan

ARTICLE INFO

Available online 20 August 2008

PACS:
78.55.Cr
61.66.Dk
68.55.Jk
78.66.Fd

Keywords:
A1. Crystal morphology
A3. Metalorganic chemical vapor deposition
B1. Nitrides
B2. Semiconducting aluminum compounds

ABSTRACT

High-reflectivity ultraviolet distributed Bragg reflectors (DBRs), based on AlN/AlGaN quarter-wave layers, have been designed and grown on 2 in (0 0 0 1) sapphire substrates by metalorganic chemical vapor deposition. The growth of 20-pair AlN/$Al_{0.23}Ga_{0.77}N$ DBR shows no observable cracks in the structure and achieves peak reflectivity of 90% at 367 nm together with a stop-band width of 24 nm. Furthermore, the growth of 34-pair AlN/$Al_{0.23}Ga_{0.77}N$ DBR shows partial cracks from optical microscopy images. According to the room-temperature photoluminescence measurement, the emission spectrum of 34-pair AlN/$Al_{0.23}Ga_{0.77}N$ DBR is broader than that of 20-pair AlN/$Al_{0.23}Ga_{0.77}N$ DBR, which could be due to strain inhomogeneity generated by cracks. Despite the crystal quality problem, the peak reflectivity of 34-pair AlN/$Al_{0.23}Ga_{0.77}N$ DBR could still achieve 97% at 358 nm and the stop-band width is 16 nm.

© 2008 Elsevier B.V. All rights reserved.

1. Introduction

High-reflectivity nitride-based distributed Bragg reflectors (DBRs) are important for the development of GaN-based optical devices such as resonant-cavity light-emitting diodes (RCLEDs) [1] and vertical-cavity surface-emitting lasers (VCSELs) [2]. Recently, nitride-based microcavity structures have attracted much attention due to the investigation of fundamental phenomena including strong light-matter interaction [3–5], solid-state cavity quantum electrodynamics (CQED) [6], and dynamical Bose–Einstein condensates [7]. As far as nitride-based microcavities designed for the study of strong coupling phenomena are concerned, the active regions made of GaN bulk or GaN/AlGaN multiple quantum wells (MQWs) are preferred due to the relatively narrow photoluminescence (PL) linewidth as compared with InGaN/GaN MQWs. Therefore, high-quality nitride-based ultraviolet DBRs with a wavelength around 360 nm at the center of the stop band are essential approach to fabricate nitride-based microcavities for the study of strong exciton–photon coupling. In general, ultraviolet nitride-based DBRs consist of AlInN/AlGaN or AlGaN/AlGaN material system. Especially, for devices containing pure GaN as an active medium, the ultraviolet DBRs cannot employ GaN as the layer materials because of the strong increases of optical absorption below 360 nm. Regarding the development of the ultraviolet DBRs for the microcavity structures made of active regions emitting in the 340–370 nm range, several experimental results have been demonstrated. Crack-free lattice-matched ultraviolet AlInN/AlGaN DBRs have been achieved by Feltin et al. [8] in 2006. The DBRs exhibit a reflectivity higher than 99% at a wavelength as short as 340 nm and a stop-band width of 20 nm. Nevertheless, the growth of high-quality AlInN film is difficult due to the composition inhomogeneity and phase separation in AlInN, which results from large mismatch of covalent bond length and growth temperature between InN and AlN [9]. High-reflectivity ultraviolet AlGaN/AlGaN DBRs with peak reflectivity of 99% are mostly grown using molecular-beam epitaxy (MBE) system [10,11]. Although the MBE system can provide high-quality epitaxial film and sharp heterostructure, it is time-consuming for the growth of high-reflectivity nitride-based DBRs as a high number of pairs are required to overcome the relatively small refractive index contrast between bilayer constituents in the nitride material system. As for AlGaN-based ultraviolet DBRs grown by metalorganic chemical vapor deposition (MOCVD) system, Wang et al. [12] have reported crack-free 25-pair AlGaN/AlGaN DBRs with a peak reflectivity of 91% at 353 nm and a stop-band width of 17 nm in 2004. Moreover, they demonstrated 25-pair AlGaN/AlGaN DBRs with peak reflectivity of 94% around 356 nm and a stop-band width of 17 nm in 2005 [13]. Ji et al. [14] reported nearly crack-free 30-pair AlGaN/AlN DBRs with a peak reflectivity of 93% at a wavelength as short as 313 nm in 2007. However, the peak reflectivity values of most AlGaN-based ultraviolet DBRs grown by MOCVD system are relatively

* Corresponding author. Tel.: +886 3 571 2121x31234; fax: +886 5 571 6631.
E-mail address: timtclu@mail.nctu.edu.tw (T.-C. Lu).

0022-0248/$ - see front matter © 2008 Elsevier B.V. All rights reserved.
doi:10.1016/j.jcrysgro.2008.08.025

lower than that grown by MBE system. Therefore, it is necessary to further improve and investigate AlGaN-based ultraviolet DBRs grown by MOCVD.

In this study, we report the growth over 2 in *c*-sapphire substrates of high-reflectivity AlN/AlGaN DBRs designed for the ultraviolet spectral region. The structures are grown by MOCVD and consist of AlN/$Al_{0.23}Ga_{0.77}N$ system to increase the difference of refractive index in the DBR structures. The measured peak reflectivity values are 90% and 97% for 20-pair and 34-pair AlN/AlGaN DBRs, respectively. Furthermore, the experimental reflectivity spectra are modeled by transfer matrix theory in order to compare the experimental and theoretical results.

2. Experiments

The AlN/AlGaN DBRs were grown in a low-pressure high-speed rotating-disk MOCVD system (EMCORE D75). Two-inch diameter (0 0 0 1)-oriented sapphire substrates were used for the growth of DBR samples. During the growth, trimethylgallium (TMGa) and trimethylaluminum (TMAl) were used as group III source materials and ammonia (NH_3) as the group V source material. After thermal cleaning of the substrate in hydrogen ambient for 5 min at 1100 °C, a 30-nm-thick GaN nucleation layer was grown at 500 °C. The growth temperature was raised up to 1020 °C for the growth of 2.8 μm GaN buffer layer. Then, the AlN/AlGaN DBRs were grown under the fixed chamber pressure of 1.33×10^4 Pa similar to the previous reported growth conditions [15]. Two DBR samples with different numbers of periods were prepared. The sample labeled DBR A consists of 20-pair AlN/$Al_{0.23}Ga_{0.77}N$ quarter-wavelength layers. The other sample labeled DBR B consists of 34-pair AlN/$Al_{0.23}Ga_{0.77}N$ quarter-wavelength layers. By employing *in situ* optical reflectivity system, the growth rate of the AlN and AlGaN layer can be estimated to be about 0.7 and 2.2 Å/s, respectively. The surface morphology of the DBRs was studied by optical microscopy and atomic force microscopy (AFM). The thicknesses of the total DBR structures were investigated by scanning electron microscopy (SEM). The reflectivity spectra of the AlN/AlGaN DBRs were measured by the *n* and *k* ultraviolet–visible spectrometer with normal incidence at room temperature [16–18]. The PL emission spectra of the DBRs were measured at room temperature in order to study the crystal quality. The excitation source is a 266 nm radiation from a frequency tripled Ti:sapphire laser and the PL emission is dispersed by a 0.55 m monochromator and detected with a photomultiplier with standard lock-in technique. The laser beam is focused by an optical objective lens and the focused laser spot size is about 50 μm together with the power density about 3×10^3 W/cm^2.

3. Results and discussion

The cross-section SEM images of DBRs A and B are shown in Fig. 1. The AlN/AlGaN interfaces are well defined and flat. According to the SEM images, the total thicknesses of 20- and 34-pair AlN/$Al_{0.23}Ga_{0.77}N$ DBRs were measured to be about 1.753 and 2.869 μm, respectively. Therefore, the average bilayer thicknesses of 87.6 nm (DBR A) and 84.4 nm (DBR B) were estimated based on the SEM measurements. Since the bilayer thickness is about 80–90 nm, the cross-sectional SEM images can provide sufficient resolution for the estimation of bilayer thicknesses [11,12,19,20]. Furthermore, by a combination of double-crystal X-ray diffraction (XRD), growth rate calibrations, and SEM measurements, we can estimate the layer thicknesses of AlN and AlGaN, respectively. For DBR A, we estimate the layer thicknesses of 45.5 nm for AlN layer and 42.1 nm for $Al_{0.23}Ga_{0.77}N$ layer. In the case of DBR B, the thicknesses of AlN and $Al_{0.23}Ga_{0.77}N$ layers are about 44.1 and 40.3 nm, respectively. Moreover, the GaN nucleation layer and GaN buffer layer can be clearly observed in Fig. 1(a).

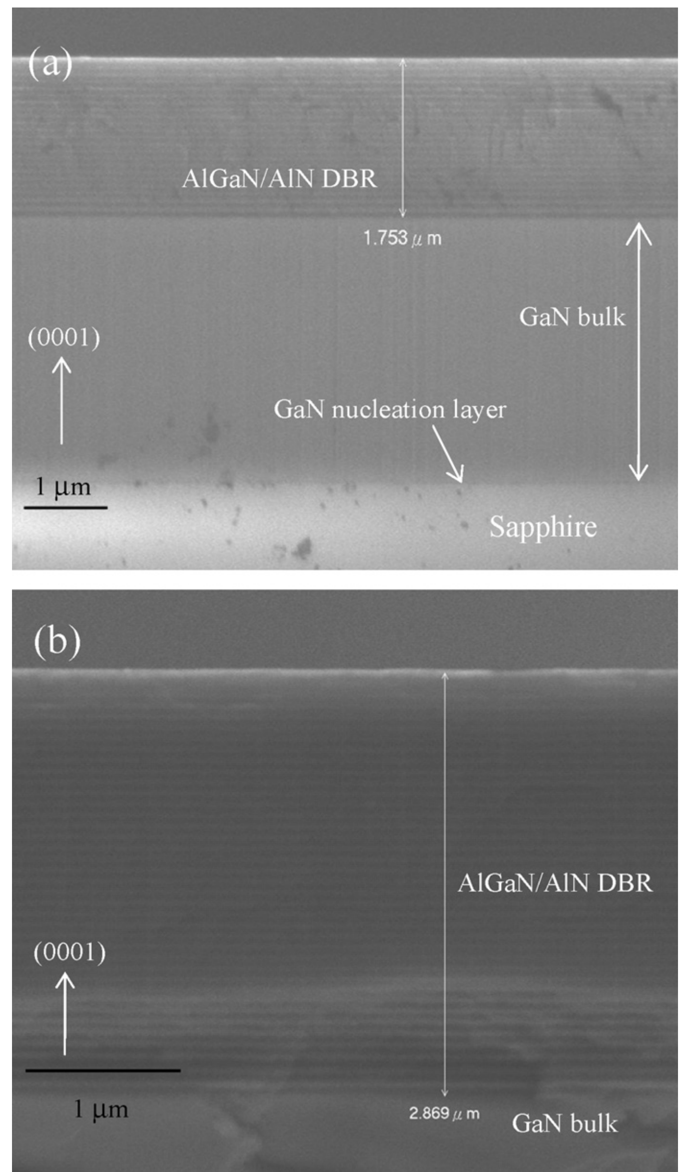

Fig. 1. (a) Cross-sectional SEM image of DBR A. The total thickness of 20-pair AlN/$Al_{0.23}Ga_{0.77}N$ DBR is about 1.753 μm. (b) Cross-sectional SEM image of DBR B. The total thickness of 34-pair AlN/$Al_{0.23}Ga_{0.77}N$ DBR is about 2.869 μm.

Fig. 2 shows the surface images of (a) DBR A and (b) DBR B taken by an optical microscopy in order to compare the macroscopic morphology between DBRs A and B. The surface image of DBR A shows a smooth macroscopic morphology but that of DBR B shows a rough one. Besides, no evidence of cracks was observed in DBR A, as shown in Fig. 2(a). As for DBR B, cracks were observed from the optical microscope image. We further estimated the mean distance between cracks of DBR B at about 300 μm. Fig. 3 shows the measured (solid line) and simulated (dashed line) reflectivity spectra of (a) DBR A and (b) DBR B. In Fig. 3(a), experimental measurement shows that the peak reflectivity at 367 nm is about 90% and the stop-band width is 24 nm. To compare experimental and calculated reflectivity spectra, theoretical simulation based on transfer matrix theory

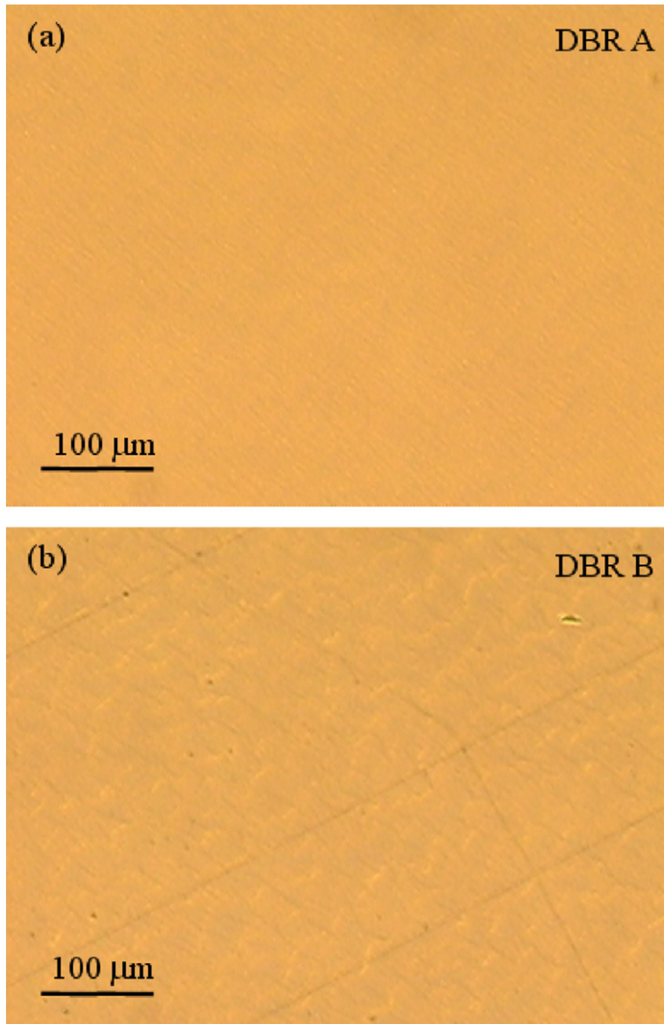

Fig. 2. Optical microscope images of (a) DBR A and (b) DBR B.

was performed using above layer thicknesses. As for the parameter of refractive index, Adachi model is employed to calculate the refractive index values of GaN, AlN, and $Al_{0.23}Ga_{0.77}N$ layers. The Adachi model can be expressed by [21]

$$n(h\nu) = \sqrt{a(x)\left(\frac{h\nu}{E_g}\right)^{-2}\left[2 - \sqrt{1 + \left(\frac{h\nu}{E_g}\right)} - \sqrt{1 - \left(\frac{h\nu}{E_g}\right)}\right] + b(x)}, \quad (1)$$

where E_g is the band gap of the material, ν is the frequency of the incident light, h is the Planck's constant, and $a(x)$ and $b(x)$ are composition-dependent fitting parameters. This equation showed good agreement with measurements on GaN, AlN, and InN for the transparency region [22]. In our calculation, we employed the fitting parameters for AlN layer from Brunner et al. [23]. As for the $Al_{0.23}Ga_{0.77}N$ layer, the fitting parameters are more reliable from Laws et al. [24] when the aluminum composition is smaller than 0.38. Fig. 3(a) also shows the calculated reflectivity spectrum of DBR A. By comparing the measured and calculated results, the characteristics of simulated reflectivity spectrum of DBR A including stop-band width and the phase of the long wavelength oscillations are in good agreement with the measured spectrum. Nevertheless, the calculated peak reflectivity is about 94%, which is larger than the measured result. This difference may come from dislocations in the samples and the structural imperfections such as deviations from the designed layer thickness and interface roughness between each epitaxial layer. Moreover, the mismatch

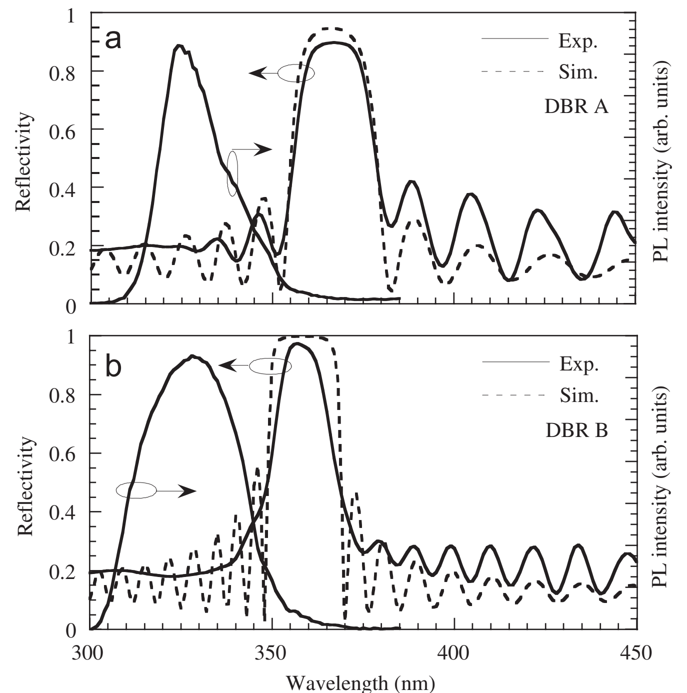

Fig. 3. (a) Measured (solid) and simulated (dashed) reflectivity spectra of DBR A at a peak wavelength of 367 nm. The room-temperature PL spectrum shows an emission peak at 323 nm from the $Al_{0.23}Ga_{0.77}N$ layers. (b) Measured (solid) and simulated (dashed) reflectivity spectra of DBR B at a peak wavelength of 358 nm. The room-temperature PL spectrum shows an emission peak at 327 nm.

between the measured and calculated reflectivity spectra in the short wavelength interference fringes is due to absorption in the $Al_{0.23}Ga_{0.77}N$ layers because the scattering loss and absorption in the bilayers were not taken into account in the simulation. In the case of DBR B, the experimental measurement shows that the peak reflectivity at 358 nm is about 97% and the stop-band width is 16 nm, as shown in Fig. 3(b). Theoretical calculation expects that the peak reflectivity and stop-band width of the 34-pair AlN/$Al_{0.23}Ga_{0.77}N$ DBRs should be 99.8% and 20 nm, respectively. Partial cracks were observed in DBR B from optical microscopy, which results from the release of the strain energy due to the large number of DBR pairs. Therefore, this difference between measured and calculated reflectivity spectra of DBR B may come from crack-induced dislocations and the degradation of crystal quality [25,26]. In addition, the short wavelength interference fringes are not resolved for DBR B. Since the stop band of DBR B is centered at a shorter wavelength than that of DBR A, the absorption effects from AlGaN layers will play a greater role in the case of DBR B as the AlGaN layers have the same aluminum composition in both samples.

In order to further observe the crystal quality and estimate the alloy compositions simultaneously, the room-temperature PL spectra of these two DBR samples were measured and also plotted in Fig. 3. The PL spectra mainly originate from the emission of AlGaN layer in DBR structures. Since the DBR samples were pumped by 266 nm laser from the top surface, the laser light will be fully absorbed by the AlGaN layers before reaching the GaN buffer layer. Therefore, the emission from GaN buffer layer cannot be observed in the PL spectra. In Fig. 3(a), the emission peak from $Al_{0.23}Ga_{0.77}N$ layer of DBR A is about 323 nm, which is obviously below the DBR stop-band wavelength range. This condition is important to keep the stop-band width in order to avoid the absorption of $Al_{0.23}Ga_{0.77}N$ layer [12]. Moreover, the emission peak from $Al_{0.23}Ga_{0.77}N$ layer of DBR B is about 327 nm, as shown in Fig. 3(b). By comparing Fig. 3(a) and (b), it is notable

that the PL spectrum of DBR B is obviously broader than that of DBR A. The full-width at half-maximum (FWHM) values of the PL spectra measured on DBRs A and B are 20.4 and 32.8 nm, respectively. Therefore, according to the broader emission spectrum and the observable cracks on sample surface, we deduce that the broader PL spectrum mainly originates from the generation of cracks, which could result in strain inhomogeneity due to the local strain depending on the distance to a crack in a cracked sample. The inhomogeneous strain distribution results in different band edge emission energy [27]. As a consequence, the tail of the emission spectrum related to the AlGaN layers in DBR B would be more extended than that in DBR A. The difference of the PL emission peak between DBRs A and B also arises from this factor since the growth condition of the $Al_{0.23}Ga_{0.77}N$ layer in DBR A and DBR B is the same.

The surface morphology of the DBR samples is investigated by AFM measurement. Fig. 4(a) and (b) are AFM images of DBRs A and B, respectively. The scanning area is $3 \times 3\,\mu m^2$. It is found that the roughness of 34-pair DBR (rms = 1.7 nm) is larger than that of 20-pair DBR (rms = 1.3 nm) within the scanning area. This larger surface roughness of DBR B may also result from the degradation of crystal quality. Rough surface morphology will lead to higher optical scattering loss, which is also one of the factors leading to the mismatch of the calculated and measured reflectivity spectra.

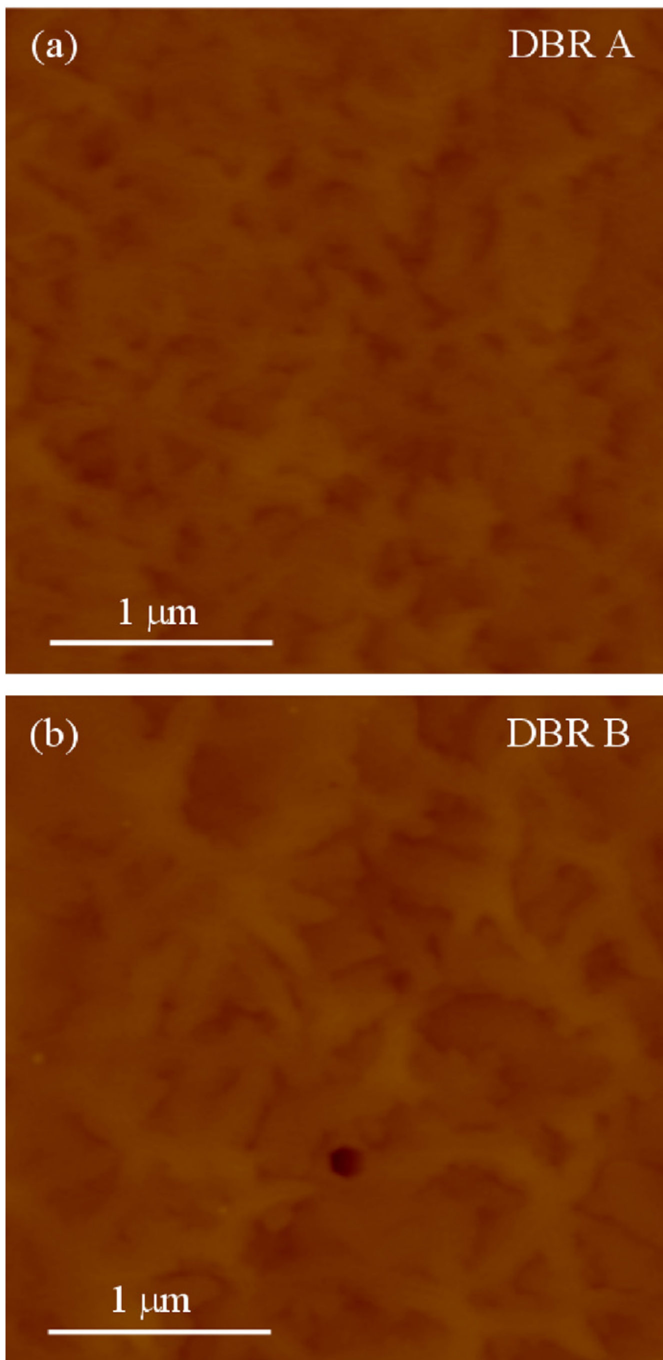

Fig. 4. AFM images ($3\,\mu m \times 3\,\mu m$) of (a) DBR A and (b) DBR B.

4. Conclusion

In summary, we have reported that the ultraviolet DBRs consist of $AlN/Al_{0.23}Ga_{0.77}N$ multilayers grown by MOCVD system. The reflectivity and stop-band width of 20-pair $AlN/Al_{0.23}Ga_{0.77}N$ DBR are 90% and 24 nm, respectively. The simulated reflectivity spectrum is in good agreement with the measured result. When the number of DBR pairs increases from 20 to 34 pairs, partial cracks are observed from optical microscopy due to the release of the strain energy. Despite the crystal quality problem, the peak reflectivity of 34-pair $AlN/Al_{0.23}Ga_{0.77}N$ DBR can still achieve 97% at a wavelength of 358 nm together with a stop-band width of 16 nm.

Acknowledgments

This work was supported in part by the National Science Council of Republic of China (ROC) in Taiwan under Contract nos. NSC 96-2221-E009-092-MY3, NSC 96-2221-E009-093-MY3, and NSC 96-2221-E009-094-MY3.

References

[1] M. Diagne, Y. He, H. Zhou, E. Makarona, A.V. Nurmikko, J. Han, K.E. Waldrip, J.J. Figiel, T. Takeuchi, M. Krames, Appl. Phys. Lett. 79 (2001) 3720.
[2] T.-C. Lu, C.-C. Kao, H.-C. Kuo, G.-S. Huang, S.-C. Wang, Appl. Phys. Lett. 92 (2008) 141102.
[3] F. Semond, I.R. Sellers, F. Natali, D. Byrne, M. Leroux, J. Massies, N. Ollier, J. Leymarie, P. Disseix, A. Vasson, Appl. Phys. Lett. 87 (2005) 021102.
[4] R. Butté, G. Christmann, E. Feltin, J.-F. Carlin, M. Mosca, M. Ilegems, N. Grandjean, Phys. Rev. B 73 (2006) 033315.
[5] G. Christmann, R. Butté, E. Feltin, J.-F. Carlin, N. Grandjean, Phys. Rev. B 73 (2006) 153305.
[6] S. Kako, C. Santori, K. Hoshino, S. Götzinger, Y. Yamamoto, Y. Arakawa, Nat. Mater. 5 (2006) 887.
[7] S. Christopoulos, G. von Högersthal, A. Grundy, P.G. Lagoudakis, A.V. Kavokin, J.J. Baumberg, G. Christmann, R. Butté, E. Feltin, J.-F. Carlin, N. Grandjean, Phys. Rev. Lett. 98 (2007) 126405.
[8] E. Feltin, J.-F. Carlin, J. Dorsaz, G. Christmann, R. Butté, M. Laügt, M. Ilegems, N. Grandjean, Appl. Phys. Lett. 88 (2006) 051108.
[9] T. Fujimori, H. Imai, A. Wakahara, H. Okada, A. Yoshida, T. Shibata, M. Tanaka, J. Crystal Growth 272 (2004) 381.
[10] O. Mitrofanov, S. Schmult, M.J. Manfra, T. Siegrist, N.G. Weimann, A.M. Sergent, R.J. Molnar, Appl. Phys. Lett. 88 (2006) 171101.
[11] A. Bhattacharya, S. Iyer, E. Iliopoulos, A.V. Sampath, J. Cabalu, T.D. Moustakas, I. Friel, J. Vac. Sci. Technol. B 20 (2002) 1229.
[12] T. Wang, R.J. Lynch, P.J. Parbrook, R. Butté, A. Alyamani, D. Sanvitto, D.M. Whittaker, M.S. Skolnick, Appl. Phys. Lett. 85 (2004) 43.
[13] A. Alyamani, D. Sanvitto, T. Wang, P.J. Parbrook, D.M. Whittaker, I.M. Ross, M.S. Skolnick, Phys. Status Solidi C 2 (2005) 813.
[14] X.-L. Ji, R.-L. Jiang, Z.-L. Xie, B. Liu, J.-J. Zhou, L. Li, P. Han, R. Zhang, Y.-D. Zheng, H.-M. Gong, Chin. Phys. Lett. 24 (2007) 1735.
[15] G.S. Huang, T.C. Lu, H.H. Yao, H.C. Kuo, S.C. Wang, C.-W. Lin, L. Chang, Appl. Phys. Lett. 88 (2006) 061904.
[16] N. Nakada, M. Nakaji, H. Ishikawa, T. Egawa, M. Umeno, T. Jimbo, Appl. Phys. Lett. 76 (2000) 1804.
[17] N. Nakada, H. Ishikawa, T. Egawa, T. Jimbo, Jpn. J. Appl. Phys. 42 (2003) L144.
[18] S.-Y. Huang, R.-H. Horng, W.-K. Wang, D.-S. Wuu, Phys. Status Solidi C 3 (2006) 2137.
[19] J.-F. Carlin, J. Dorsaz, E. Feltin, R. Butté, N. Grandjean, M. Ilegems, M. Laügt, Appl. Phys. Lett. 86 (2005) 031107.

[20] H.M. Ng, T.D. Moustakas, S.N.G. Chu, Appl. Phys. Lett. 76 (2000) 2818.
[21] S. Adachi, Physical Properties of III–V Semiconductor Compounds, Wiley, New York, 1992.
[22] T. Peng, J. Piprek, Electron. Lett. 32 (1996) 2285.
[23] D. Brunner, H. Angerer, E. Bustarret, F. Freudenberg, R. Höpler, R. Dimitrov, O. Ambacher, M. Stutzmann, J. Appl. Phys. 82 (1997) 5090.
[24] G.M. Laws, E.C. Larkins, I. Harrison, C. Molloy, D. Somerford, J. Appl. Phys. 89 (2001) 1108.
[25] S.J. Hearne, J. Han, S.R. Lee, J.A. Floro, D.M. Follstaedt, E. Chason, I.S.T. Tsong, Appl. Phys. Lett. 76 (2000) 1534.
[26] J.A. Floro, D.M. Follstaedt, P. Provencio, S.J. Hearne, S.R. Lee, J. Appl. Phys. 96 (2004) 7087.
[27] B. Gil, O. Briot, R.-L. Aulombard, Phys. Rev. B 52 (1995) R17028.